Materials Research. 2024; 27(suppl. 1):e20230560
DOI: https://doi.org/10.1590/1980-5373-MR-2023-0560

Localized Corrosion Resistance Assessment of 11 Alloys in the Presence of DBNPA Biocide: A Material Compatibility Study

***Luan C. Santos*[a*], *Rhuãn C. Souza*[b], *Gabriela P.C. Moreira*[a], *Carlos E.V. Masalla*[c], *Jefferson R. Oliveira*[d], *Guillermo Vilalta-Alonso*[b], *Alysson H.S. Bueno*[b]**

[a]*Universidade Federal de São João Del-Rei (UFSJ), Programa de Pós-Graduação em Física e Química de Materiais (FQMAT), São João del Rei, MG, Brasil.*
[b]*Universidade Federal de São João Del-Rei (UFSJ), Departamento de Engenharia Mecânica (DEMEC), São João del Rei, MG, Brasil.*
[c]*Universidade Federal de São João Del-Rei (UFSJ), Programa de Pós-Graduação em Engenharia Mecânica (PPMEC), São João del Rei, MG, Brasil.*
[d]*Petrobras S.A., Rio de Janeiro, RJ, Brasil.*

Received: December 18, 2023; Revised: March 21, 2023; Accepted: April 23, 2024

Microbiologically influenced corrosion is a common problem in the oil and gas industry. It is a type of corrosion induced by biofilm-forming microorganisms such as sulfate-reducing bacteria which produces corrosive compounds as a product of their respiration. The most indicated treatment for the issue is the use of biocides, chemical substances used to kill microbes. However, biocides are corrosive to many materials, making their selection a problem. The 2,2-dibromopropanediamide (BDNPA) is a biocide used to control the growth of a wide range microorganisms. There is a literature gap for selecting materials that can be used with DBNPA Biocide without risk of corrosion. Hence, this research is dedicated to investigating the corrosion behaviour of commonly used alloys in a DBNPA solution. This work evaluated 11 alloys commonly used in the laboratory for the manufacture of instrumentation piping. Anodic polarization tests and 30 days immersion tests were carried out in a 100% DBNPA solution at two temperatures (25 and 40 ºC). Among the analysed alloys, only 4 were approved by the tests in all tested temperature ranges (Titanium Grade 2, Hastelloy C276, Inconel 625 and Superduplex Steel SAF 2507). These alloys did not present a localized corrosion process in any of the 30-day immersion tests, in addition, they obtained a significant passivation domain in the anodic polarization test at 40 ºC. The remaining alloys (AISI 304, AISI 316, AISI 317, AISI 321, AISI 347, Monel 400) were not approved in all temperature ranges tested for transport and storage of 100% BDNPA biocide solution.

Keywords: *Localized corrosion, Biocides, DBNPA.*

1. Introduction

In recent decades, the continuous development of the oil and gas industry has created a scenario where the safe production and transportation of oil is extremely important, making the corrosion of infrastructures a serious problem[1].

According to estimates by the National Association of Corrosion Engineers (NACE), the cost of corrosion in the United States is approximately $500 billion per year. This includes direct costs, such as repairs or replacement of corroded infrastructure, as well as indirect costs, such as lost productivity and environmental cleanup[2].

In the context of offshore oil exploration, external corrosion is a common problem, being a type of corrosion that occurs on the external surface of oil pipelines. One of the main mechanisms causing external corrosion in oil pipelines is microbiologically influenced corrosion (MIC). MIC has been identified in pipelines in a wide variety of soils where microorganisms such as sulphate-reducing bacteria (SRB) exist. These bacteria are anaerobic and can reduce sulphates to hydrogen sulphide (H_2S), which cause corrosion in metal structures and piping[3]. MIC can accelerate uniform corrosion and induce localized corrosion of carbon steels and stainless steels[4].

Treatment using oxidizing or non-oxidizing biocides is a traditional method to control MIC in addition to physical purification (or pigging)[5]. The 2,2-dibromo-3-nitrilopropionamide (DBNPA), a fast-killing, non-oxidizing, broad-spectrum, biocide is commonly used on oil rigs to

*e-mail: luancarrerasantos@gmail.com

mitigate the effects of MIC. DBNPA can react with sulphur-containing nucleophiles thereby disrupting the biological functions of bacteria by killing them.

However, DBNPA has a downside. Its low pH and the intermediate products of its dissociation can corrode the equipment in which it operates[6]. These intermediates can form through chemical reactions between the biocide and other substances in the environment, such as dissolved salts, or through the degradation of the biocide itself when exposed to sunlight[7]. Also, DBNPA can undergo hydrolysis, resulting in the formation of dibromoacetic acid and dibromoacetonitrile as its primary products[8].

In contrast, passive alloys are designed to resist corrosion through the creation of an oxygen-rich passive film[9,10]. Although, this protective layer can be compromised by halide ions such as bromine, which is a byproduct of the DBNPA's chemical breakdown process. This compromise can instigate a localized attack on the alloy. This typically occur when bromine or chlorine ions interact with the alloy surface.

This interaction triggers the formation of bromine compounds with the iron present in the alloy, leading to the manifestation of pits or cracks on the metal surface. These deformations are indicative of corrosion, highlighting the potential detrimental effects of DBNPA's byproducts on passive alloys[11]. Hence, when stored in its undiluted form (100% concentration) over extended periods, DBNPA can cause corrosion issues in storage tanks and transportation pipes.

Furthermore, in the event of pipeline leaks or ruptures, the biocide can inadvertently be released into the environment. This accidental release can result in the pollution of water, soil, and air, further emphasizing the need for careful handling and storage of DBNPA. This not only has detrimental effects on the environment but can also pose significant risks to human health. The US regulatory agency categorizes DBNPA as corrosive to the eyes, placing it in toxicity category I, the most severe of the four acute toxicity categories. It is also considered moderately toxic systemically via oral or inhalation exposure (toxicity category II), and mildly toxic through dermal exposure (toxicity category III)[12].

Biocides, such as 2,2-dibromo-3-nitrilopropionamide (DBNPA), are instrumental in inhibiting microbial growth across a range of industrial applications. However, a review of existing literature indicates a noticeable absence of thorough studies investigating the corrosive impacts of these biocides on various alloys when stored in their pure, undiluted state. Most studies[5,6,12,13] focus on its effect on microorganism colonies and their environmental impact. This literature gap underscores the pressing need for in-depth investigations that not only elucidate the corrosion mechanisms but also guide informed material choices to ensure the long-term integrity of industrial systems employing DBNPA as a biocide. This research primarily focuses on examining the resistance of eleven unique alloys, commonly used in the pipeline industry, to localized corrosion. The aim is to aid in the selection of appropriate materials for the conveyance and storage of the biocide DBNPA.

2. Metodology

This study examined the resistance to localized corrosion of eleven different alloys, which are commonly used in industrial applications. The selection was made to assess their corrosion resistance in the presence of the DBNPA biocide. The alloys chosen represent a broad range of materials, including AISI 304, AISI 316, AISI 317, AISI 321, AISI 347, Monel 400, Inconel 625, Superduplex SAF 2507, Duplex SAF 2205, Hastelloy C276, and Titanium Grade 2. The evaluated metallurgy and their compositions, expressed in weight percentages, are presented in Tables 1, 2, and 3.

Laboratory examinations were conducted in compliance with ASTM G1, ASTM G-5, ASTM G-31, and ASTM G-46 standards. Both anodic potentiodynamic polarization and immersion tests were performed thrice under two different temperatures: room temperature (25 °C) and 40 °C. To exclusively study the corrosive impact of DBNPA and to mimic the industrial conditions of storage and transportation, all tests employed a solution of 100% 2,2-dibromo-3-nitrilopropionamide in an aerated state.

3. Anodic Potentiodynamic Polarization Tests

The anodic potentiodynamic polarization used an AUTOLAB model multipotentiostat: Autolab type III/FRA2 connected to a computer with the NOVA 1.11.2 software and a conventional 3-electrode electrochemical cell (working electrode, platinum counter electrode and saturated calomel). The scanning speed used was 0.000167 V/s and the exposure area of the specimens was 1 cm^2 in accordance with the standard used. The specimens were sanded down to 600 grit sandpaper, then washed with distilled water and acetone and dried with hot air. Soon after, the samples were soldered on a wire to allow the application of potential, then they were isolated using liquid insulating tape.

3.1. Immersion tests

For the immersion tests, the specimens were initially sanded down to a 120-grit finish, followed by a thorough cleaning with distilled water and acetone. After drying with hot air, the samples were wrapped in paper and stored in a vacuum desiccator to prevent contamination.

Table 1. Chemical Composition of nickel alloys.

Alloying Element	Hastelloy C276	Inconel 625	Monel 400
Al (%p)	--	0.040	--
C (%p)	0.010	0.060	0.010
Co (%p)	2.500	1.000	--
Cr (%p)	14.500 - 16.500	21.000	--
Cu (%p)	--	--	32.000 - 33.000
Fe (%p)	4.000 - 7.000	5.000	1.000 - 2.000
Nb (%p)	--	3.500	
Ni (%p)	57.000	62.000	63.000 – 65.000
Mn (%p)	1.000	--	--
Mo (%p)	15.000 – 17.000	9.000	--
P (%p)	0.030	--	--
S (%p)	0.010	--	--
Si (%p)	0.080	--	--
Ti (%p)	--	0.270	--
V (%p)	0.350	--	--
W (%p)	3.000 - 4.500	--	--

The testing procedure involved completely immersing the specimens in a 100% BDNPA biocide solution at the specified temperature. Beakers of 400 ml and 500 ml, available in the laboratory, were used to hold the solution. Three specimens of identical material were placed in each beaker using Teflon wires affixed to the beaker. These beakers were then positioned in water baths filled with distilled water. The temperature of the biocide was monitored using an analog thermometer until the desired reading was achieved.

3.2. Characterization and evaluation of the incidence of corrosion by pitting

As per ASTM G-46, the loss of metal mass is typically not recommended as a metric for assessing the extent of corrosion, unless the overall corrosion is mild and pitting is significantly severe. If the corrosion is uniform and substantial, the contribution of pitting to the total metal loss is minimal, making it challenging to accurately determine the corrosion damage from the mass loss. Consequently, the incidence of corrosion was evaluated based on the density of pits. To facilitate the calculation of pit density in the samples, electronic micrographs were produced using a HITACHI microscope, model TM 3000, operating at a voltage of 15 kV with magnification levels ranging from 100 to 4000x. Following ASTM G-46 standard, an area of 0.6 cm^2 was selected for the counting and calculation of pit density.

Table 2. Chemical composition of Titanium Grade 2.

Chemical composition Titanium Grade 2	
C (%p)	0.080
Fe (%p)	0.250
H (%p)	0.015
N (%p)	0.030
O (%p)	0.250
Other (%p)	0.400
Ti (%p)	98.270

4. Results

4.1. Potentiodynamic polarization tests

In this section, the outcomes of the potentiodynamic polarization tests conducted on each material are presented. These tests were performed at two distinct temperatures, 25 ºC and 40 °C, in a solution consisting entirely of BDNPA biocide. All tests were reliably reproduced in triplicate. The results will be displayed in a sequence, starting from the most noble alloy and concluding with the least noble one.

4.1.1. Titanium grade 2

Upon analysis of Figure 1 and Table 4, it is evident that Titanium exhibited a passivation domain across the entire spectrum of the applied anodic potential. There was no observation of pitting potential, and the current density consistently remained below 1×10^{-05} A/cm^2. This is indicative of a passivation process devoid of anodic dissolution on the metal surface. Given that Titanium demonstrated resistance

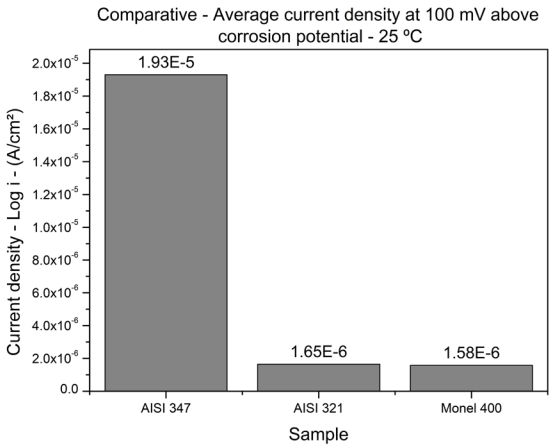

Figure 1. Anodic polarization curve of Grade 2 Titanium at a temperature of 40 ºC in a 100% BDNPA biocide solution.

Table 3. Chemical composition - Stainless steels.

Alloying Element	Super duplex SAF 2507	Duplex SAF 2205	AISI 347	AISI 321	AISI 317	AISI 316	AISI 304
C (%p)	0.030	0.030	0.080	0.080	0.080	0.080	0.080
Cr (%p)	25.000	22.500	17.000-	17.000-	18.000-	16.000-	18.000-
			19.500	19.000	20.000	18.000	20.000
Cu (%p)	0.500	--	--	--	--	--	--
Fe (%p)	61.100	65.500	64.000	66.000	57.850-	61.800-	66.345-
					68.000	72.000	74.000
Mn (%p)	1.200	2.000	2.000	2.000	2.000	2.000	2.000
Mo (%p)	4.000	3.200	--	--	3.000-	2.000-	--
					4.000	3.000	
N (%p)	0.300	0.180	--	--	--	--	--
Ni (%p)	7.000	5.500	9.000-	9.000-	11.000-	10.000-	8.000-
			13.000	12.000	15.000	14.000	10.500
P (%p)	0.035	0.030	0.040	0.040	0.045	0.045	0.045
S (%p)	0.015	0.015	0.030	0.030	0.030	0.030	--
Si (%p)	0.800	1.000	1.000	1.000	1.000	1.000	1.000

to pitting corrosion at a temperature of 40 °C, there was no necessity to conduct anodic polarization tests at room temperature.

4.1.2. Inconel 625

Upon analysis of Table 5 and Figure 2, it is evident that the corrosion potential tended to increase from the ambient temperature to 40 ºC, indicating a passive film formation process that is accelerated as the temperature increases. An increase in pitting potential is also noted at a temperature of 40 ºC. The passivation domain remained similar at both temperatures. It is inferred that in the conditions analysed, the pitting corrosion resistance of Inconel 625 was not significantly affected by the variation of temperature.

4.1.3. Hastelloy C276

From Table 6 and Figure 3, it's observed that as temperature rises, corrosion potential increases, indicating an accelerated passive film formation. Concurrently, pitting potential decreases, suggesting a lower anode potential can disrupt material passivation. Despite a reduced passivation domain with higher temperatures, the minor variations suggest that the pitting corrosion resistance of Hastelloy C276 is minimally affected within the tested temperature ranges.

4.1.4. Superduplex stainless steel SAF 2507

Upon examining Table 7 and Figure 4, it can be observed that the corrosion potential tends to rise with an increase in temperature. This trend suggests that the process of passive film formation likely accelerates as the temperature rises. As the temperature increases, a decrease in pitting potential is noted. In this scenario, a lower applied anode potential was sufficient to disrupt the passivation of the material with the temperature increase. Temperature exerted a significant influence on the passivation domain, particularly when compared to the Inconel 625 and Hastelloy C276 alloys. For the Superduplex SAF 2507 steel, the decline in the passive domain represented a difference of 55% between the conditions at 25 ºC and 40 ºC.

4.1.5. Duplex stainless steel SAF 2205

Analysing Table 8 and Figure 5 it is possible to observe that the corrosion potential tended to increase with the

Table 4. Average corrosion potential obtained from anodic polarization curves of Grade 2 Titanium in 100% BDNPA biocide solution.

Temperature (ºC)	Medium corrosion potential (V)
40 ºC	0.011 ±0.0282

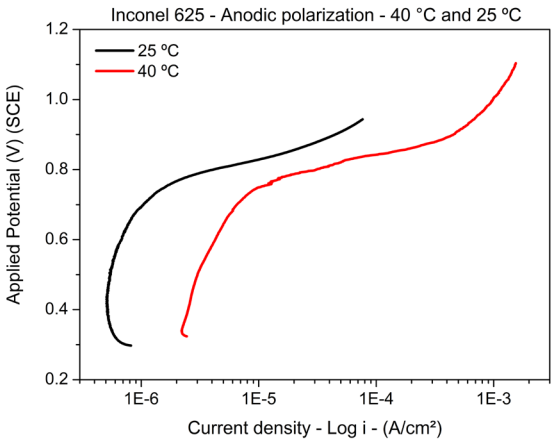

Figure 2. Anodic polarization curves of Inconel 625 at 40 °C and 25 ºC in a 100% BDNPA biocide solution.

Table 5. Average corrosion potential, pitting potential and passivation domain obtained from the anodic polarization curves of Inconel 625 in 100% BDNPA biocide solution.

Temperature (ºC)	Medium corrosion potential (V)	Medium Pitting Potential (V)	Medium Passivation Domain (V) |Pitting potential – |Corrosion pot. |
25 ºC	0.298 ±0.029	0.703±0.006	0.405 ±0.030
40 ºC	0.336 ±0.028	0.747 ±0.005	0.410 ±0.027

Table 6. Average corrosion potential, pitting potential and passivation domain obtained from the anodic polarization curves of Hastelloy C276 in 100% BDNPA biocide solution.

Temperature (ºC)	Medium corrosion potential (V)	Medium Pitting Potential (V)	Medium Passivation Domain (V) |Pitting potential – |Corrosion pot. |
25 ºC	0.275 ±0.005	0.723 ±0.012	0.447 ±0.016
40 ºC	0.296 ±0.023	0.706 ±0.005	0.410 ±0.005

Table 7. Average corrosion potential, pitting potential and passivation domain obtained from the anodic polarization curves of Superduplex Stainless Steel SAF 2507 in 100% BDNPA biocide solution.

Temperature (ºC)	Medium corrosion potential (V)	Medium Pitting Potential (V)	Medium Passivation Domain (V) |Pitting potential – |Corrosion pot. |
25 ºC	0.215 ±0.034	0.660 ±0.015	0.481 ±0.046
40 ºC	0.292 ±0.044	0.493 ±0.021	0.225 ±0.039

increase in temperature, having great influence on the resistance to pitting corrosion of Duplex SAF 2205 steel. It is observed that the steel presented a passivation domain only in tests at room temperature. At 40 ºC, Duplex SAF 2205 steel showed active dissolution, with no passivation domain observed in the applied anodic potential range. This behaviour highlights the lower resistance to pitting corrosion of this steel when compared to the Superduplex steel alloys SAF 2507, Hastelloy C276, Inconel 625 and Titanium Grade 2.

4.1.6. Stainless steel AISI 347

Figure 6 and Table 9 show that AISI 347 steel presented a drop in corrosion potential as the temperature increased. This behaviour is probably due to the temperature having intensified the corrosive process on the metal surface, increasing the kinetics of electrochemical reactions. At both temperatures tested, AISI 347 steel showed active dissolution, with no passivation domain observed in the applied anodic potential range. Analysing the current density at 100 mV above the corrosion potential, as the temperature increases,

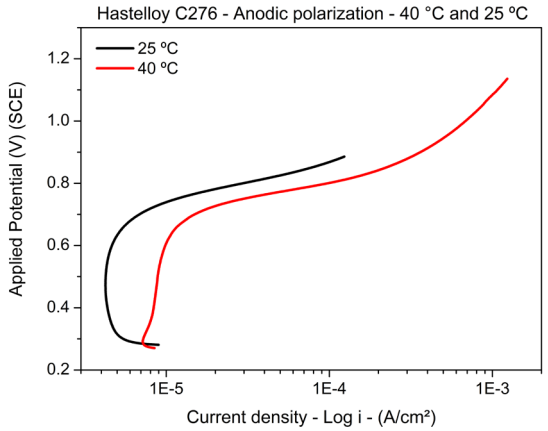

Figure 3. Anodic polarization curves of Hastelloy C276 at 40 °C and 25 ºC in a 100% BDNPA biocide solution.

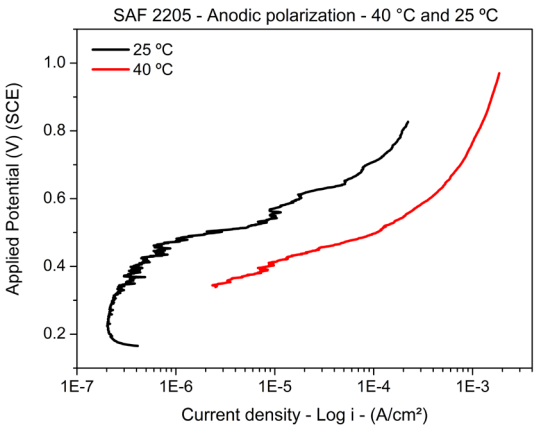

Figure 5. Anodic polarization curves of Duplex Stainless Steel SAF 2205 at 40 °C and 25 ºC in a 100% BDNPA biocide solution.

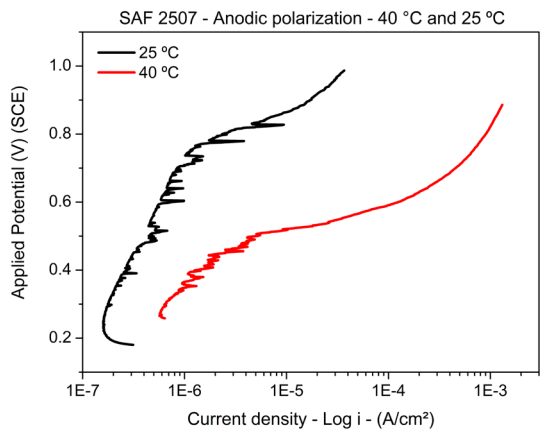

Figure 4. Anodic polarization curves of Superduplex Stainless Steel SAF 2507 at 40 °C and 25 ºC in a 100% BDNPA biocide solution.

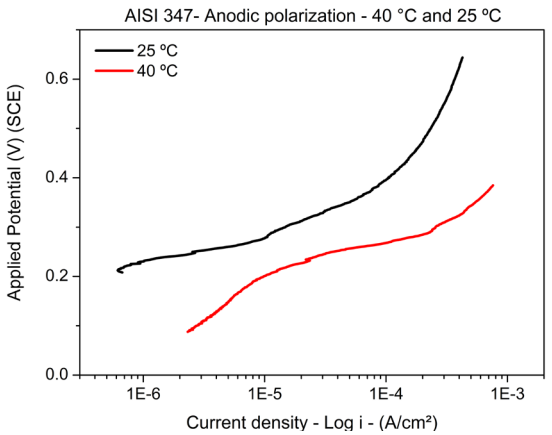

Figure 6. Anodic polarization curves of Stainless Steel AISI 347 at 40 °C and 25 ºC in a 100% BDNPA biocide solution.

Table 8. Average corrosion potential, pitting potential and passivation domain obtained from the anodic polarization curves of Duplex Stainless Steel SAF 2205 in 100% BDNPA biocide solution.

Temperature (ºC)	Medium corrosion potential (V)	Medium Pitting Potential (V)	Medium Passivation Domain (V) |Pitting potential – |Corrosion pot. |	Current Density 100 mV Above Corrosion Pot. (medium) (A/cm²)
25 ºC	0.248 ±0.082	0.380 ±0.021	0.135 ±0.098	3.830E-07 ±1.332E-07
40 ºC	0.324 ±0.068	Active Dissolution	Active Dissolution	8.320E-06 ±1.065E-05

the current density increases, result of a stronger corrosion process. A difference of one decimal order was observed between room temperature and the 40 ºC condition.

4.1.7. Stainless steel AISI 321

Figure 7 and Table 10 show that the corrosion potential increased with increasing temperature. All conditions showed active dissolution in the applied anodic potential range. Analysing the current densities at 100 mV above the corrosion potential, as the temperature increased, the more aggressive the corrosive process became, as observed by the increase in current densities. A difference of two decimal orders was observed between room temperature and the 40 ºC condition.

4.1.8. Stainless steel AISI 317

Figure 8 and Table 11 show that at a temperature of 40 °C, AISI 317 steel showed active dissolution throughout the entire range of applied anode potential. Not being qualified to work from this temperature of 40 °C with this BDNPA biocide. Analysing the current densities at 100 mV above the corrosion potential it is verified that as the temperature increases the current densities also increase, for the passivation conditions a difference of one decimal order in the current density is observed.

4.1.9. Stainless steel AISI 316

Figure 9 and Table 12 show that for the 40 ºC condition, the corrosion potential became more positive, and the material showed active dissolution across the entire range of applied anodic potential, highlighting the influence of temperature in accelerating the corrosive process of AISI 316 steel with the biocide BDNPA. Analysing the current density at 100 mV above the corrosion potential, as the temperature increases, the current density increases, making the corrosion process more aggressive. A difference of two decimal orders was observed between the ambient temperature and the condition of 40 ºC.

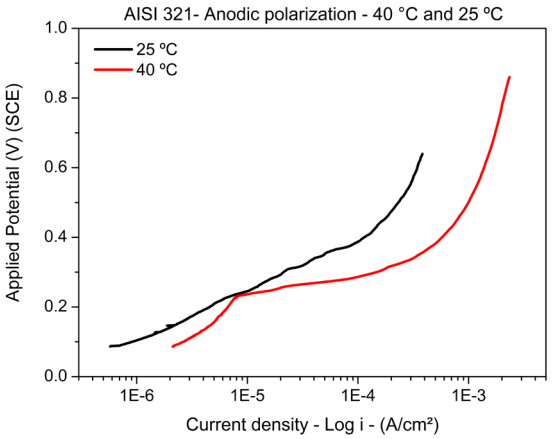

Figure 7. Anodic polarization curves of Stainless Steel AISI 321 at 40 °C and 25 ºC in a 100% BDNPA biocide solution.

Table 9. Average corrosion potential, pitting potential and passivation domain obtained from the anodic polarization curves of Stainless Steel AISI 347 in 100% BDNPA biocide solution.

Temperature (ºC)	Medium corrosion potential (V)	Current Density 100mV Above Corrosion Pot. (medium) (A/cm²)
25 ºC	0.270 ±0.0684	1.93E-05 ±7.962E-06
40 ºC	0.053 ±0.0311	7.14E-06 ±2.451 E-06

Table 10. Average corrosion potential, pitting potential and passivation domain obtained from the anodic polarization curves of Stainless Steel AISI 321 in 100% BDNPA biocide solution.

Temperature (ºC)	Medium corrosion potential (V)	Current Density 100 mV Above Corrosion Pot. (medium) (A/cm²)
25 ºC	0.176 ±0.0095	1.650E-06 ±4.98E-07
40 ºC	0.387 ±0.0180	5.540E-04 ±4.053E-04

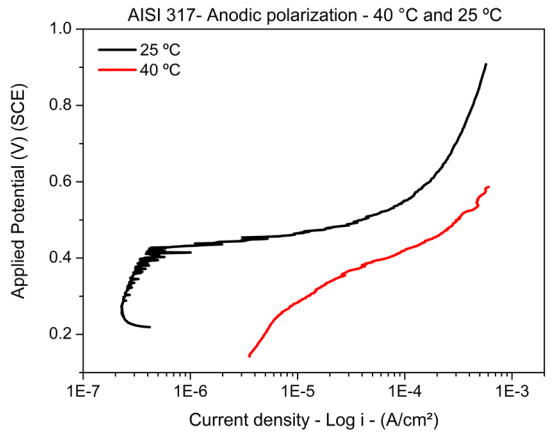

Figure 8. Anodic polarization curves of Stainless Steel AISI 317 at 40 °C and 25 ºC in a 100% BDNPA biocide solution.

Table 11. Corrosion potential, pitting potential, passivation domain and current density at 100 mV above corrosion potential obtained from the anodic polarization curves of AISI 317 in 100% BDNPA biocide solution.

Temperature (ºC)	Medium corrosion potential (V)	Medium Pitting Potential (V)	Medium Passivation Domain (V) |Pitting potential – |Corrosion pot. |	Current Density 100 mV Above Corrosion Pot. (medium) (A/cm²)
25 ºC	0.267 ±0.047	0.42 ±0.05	0.159 ±0.0438	5.140E-07±2.409E-07
40 ºC	0.145 ±0.0239	Active Dissolution	Active Dissolution	5.560E-06 ±1.972E-06

Table 12. Corrosion potential, pitting potential, passivation domain and current density at 100 mV above corrosion potential obtained from the anodic polarization curves of AISI 313 in 100% BDNPA biocide solution.

Temperature (ºC)	Medium corrosion potential (V)	Medium Pitting Potential (V)	Medium Passivation Domain (V) |Pitting potential – |Corrosion pot. |	Current Density 100 mV Above Corrosion Pot. (medium) (A/cm²)
25 ºC	0.195±0.042	0.307 ±0.0057	0.111 ±0.048	8.120E-06 ±1.340E-06
40 ºC	0.268 ±0.062	Dissolução Ativa	Dissolução Ativa	3.710E-04 ±2.220E-04

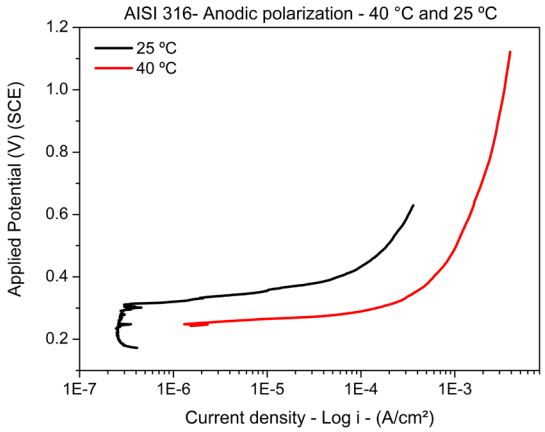

Figure 9. Anodic polarization curves of Stainless Steel AISI 316 at 40 °C and 25 ºC in a 100% BDNPA biocide solution.

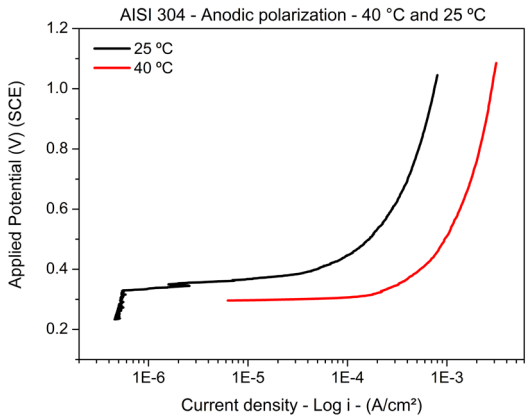

Figure 10. Anodic polarization curves of Stainless Steel AISI 304 at 40 °C and 25 ºC in a 100% BDNPA biocide solution.

4.1.10. Stainless steel AISI 304

Upon analysing Figure 10 and Table 13, at 25 ºC, a pseudopassivation process was noted with the metal showing minor initial resistance but no passive domain. All tested conditions exhibited active dissolution. As temperature rose, current densities increased, indicating an intensified corrosive process. A decimal difference was observed between room temperature and the 40 ºC condition.

Table 13. Corrosion potential and current density at 100 mV above the average corrosion potential obtained from the anodic polarization curves of AISI 304 in a 100% BDNPA biocide solution.

Temperature (ºC)	Medium corrosion potential (V)	Current Density 100mV Above Corrosion Pot. (medium) (A/cm²)
25 ºC	0.176 ±0.0095	1.650E-06 ±1.958E-06
40 ºC	0.336 ±0.0280	4.83E-04 ±5.939E-05

Table 14. Corrosion potential and current density at 100 mV above the average corrosion potential obtained from the anodic polarization curves of AISI 304 in a 100% BDNPA biocide solution.

Temperature (ºC)	Medium corrosion potential (V)	Current Density 100 mV Above Corrosion Pot. (medium) (A/cm²)
25 ºC	0.176 ±0.0095	1.580E-06 ±1.871E-06
40 ºC	0.0404 ±0.0344	6.52E-04 ±7.215E-05

4.1.11. Monel 400

Upon analysing Figure 11 and Table 14, both conditions showed active dissolution in the applied anodic potential range. Analysing the current densities at 100 mV above the corrosion potential, as the temperature increased, the more aggressive the corrosive process became, resulting in an increase in current densities.

4.2. Immersion Tests

The results of the 30-day immersion tests in a 100% BDNPA Biocide solution are presented below. The alloys Titanium Grade 2, Inconel 625, Hastelloy C276, Superduplex SAF 2507, Duplex SAF 2205, did not present any sign of localized corrosion after 30 days of immersion in a 100% BDNPA biocide solution in both temperatures. Hence no SEM images of these materials will be present.

4.2.1. Characterization and assessment of the incidence of pitting corrosion in metallurgy

4.2.1.1. Stainless steel AISI 347

Analysing Figure 12, it is possible to observe that AISI 347 Steel showed pitting after 30 days of immersion at 40 ºC

in a 100% BDNPA biocide solution. The pitting density was 1.7x10^{06} pit/m^2 for this condition. The AISI 347 Steel did not develop pits at 25 ºC after 30 days of immersion in a 100% BDNPA biocide solution, showing no apparent corrosive process.

4.2.1.2. Stainless steel AISI 321

The AISI 321 Steel showed a localized corrosion process after 30 days of immersion in all tested conditions (Figures 13 and 14). For the room temperature condition, the pitting corrosion process was reduced, but small pits appeared (Figure 14). This result is corroborated by anodic polarization tests in which AISI 321 Steel showed active dissolution in all tested conditions.

For a temperature of 40 ºC the density of pits was 2.84 x10^{06} pit/m^2, for a temperature of 25 ºC condition the value was 1.25 x 10^{05} pit/m^2. Therefore, it is concluded that there is a reduction in the intensity of the corrosive process with the reduction in temperature.

4.2.1.3. Stainless steel AISI 317

Analyzing Figure 15, it is possible to observe that AISI 317 Steel showed pitting after 30 days of immersion at 40 ºC in a 100% BDNPA biocide solution. The pitting density was 1.25 x 10^{05} pit/m^2 for this condition. The AISI 317 Steel did not develop pits at a temperature of 25 ºC. The results of the anodic polarizations of the material corroborate these results, in which the AISI 317 Steel presented a domain of passivation under conditions of 25 ºC.

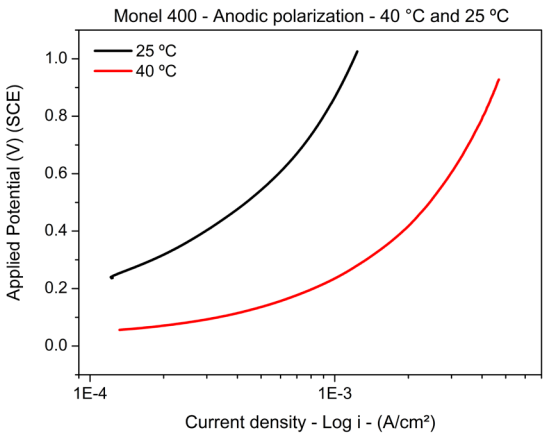

Figure 11. Anodic polarization curves of Monel 400 at 40 °C and 25 ºC in a 100% BDNPA biocide solution.

4.2.1.4. Stainless steel AISI 316

AISI 316 Steel showed a localized corrosion process after 30 days of immersion in all tested conditions (Figures 16, 17). For the 25 ºC temperature condition, the corrosion process was reduced, but small pits appeared. For a temperature of 40 ºC the density of pits was 6.1 x 10^{06} pit/m^2 and for 25 ºC temperature 3.1 x 10^{05} pit/m^2. A reduction in the intensity of the corrosive process is noted with the reduction in temperature.

4.2.1.5. Stainless steel AISI 304

AISI 304 Steel showed a localized corrosion process after 30 days of immersion in all tested conditions (Figure 18 and 19). For a temperature of 40 ºC the density of pits was 3.7 x 10^{05} pit/m^2, and for 25 ºC temperature 1.25 x 10^{05} pit/m^2. A reduction in the intensity of the corrosive process is noted with the reduction in temperature.

4.2.1.6. Monel 400

It is possible to observe that Monel 400 showed a generalized corrosion process after 30 days of immersion in all tested conditions (Figure 20 and 21). The result is corroborated by the anodic polarization tests in which Monel 400 showed an active dissolution process in all tested conditions.

5. Discussion

In this section, the results of anodic polarizations and immersion tests between materials will be compared according to temperature.

According to Figure 22, it is observed that Titanium Grade 2 is the metal that has the highest passivation domain at 40 °C, then Hastelloy C276 and Inconel 625 steels have a similar passive domain, however 72% smaller than the one found for Grade 2 Titanium, showing the superior corrosion resistance of the titanium alloy element. Furthermore,

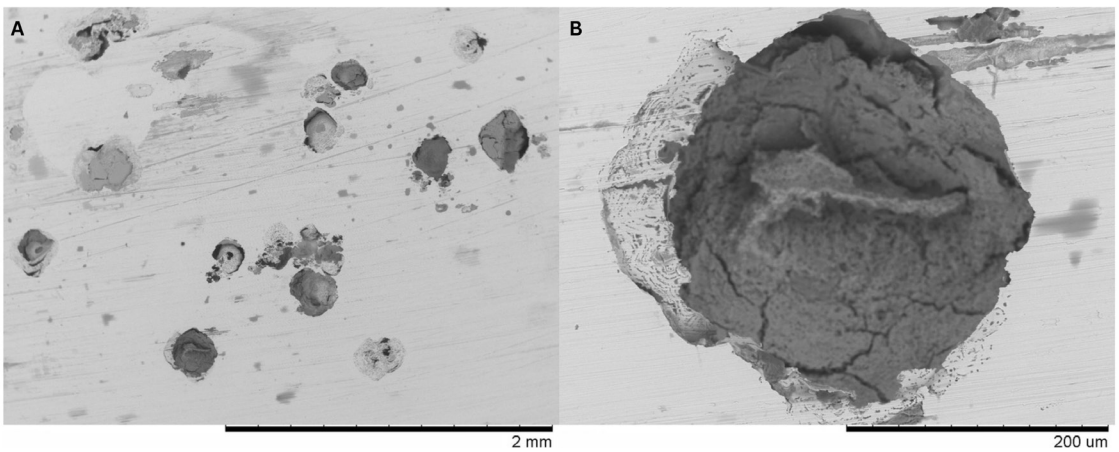

Figure 12. Characterization (SEM) of a sample of AISI 347 Steel after immersion for 30 days at 40 ºC (a) 50x (b) 500x.

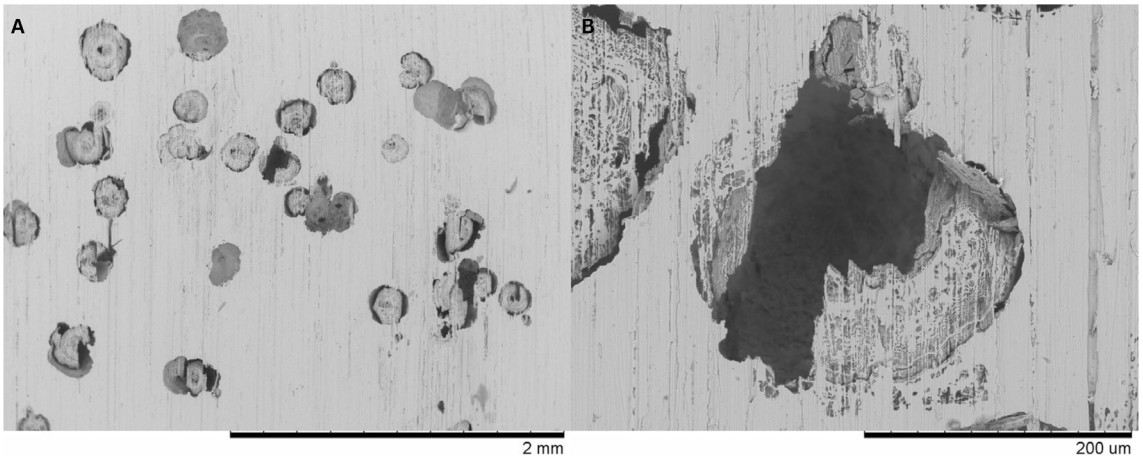

Figure 13. Characterization (SEM) of a sample of AISI 321 Steel after immersion for 30 days at 40 ºC. (a) 50x (b) 500x.

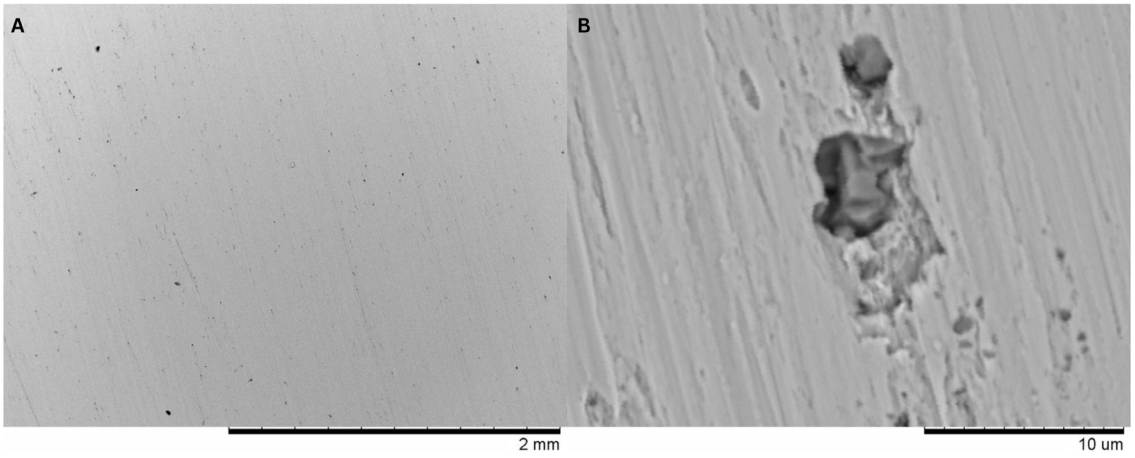

Figure 14. Characterization (SEM) of a sample of AISI 321 Steel after immersion for 30 days at 25 ºC. (a) 50x (b) 500x.

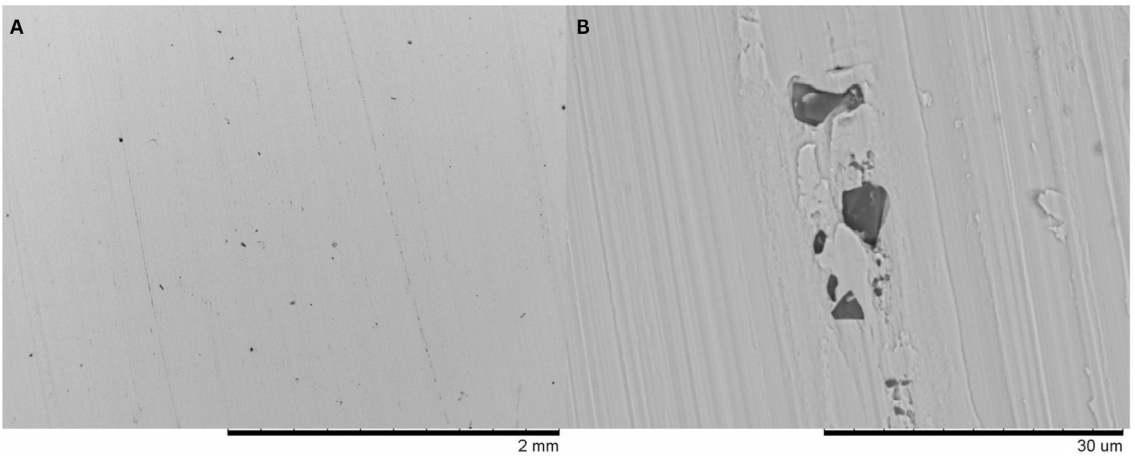

Figure 15. Characterization (SEM) of a sample of AISI 317 Steel after immersion for 30 days at 40 ºC. (a) 50x (b) 500x.

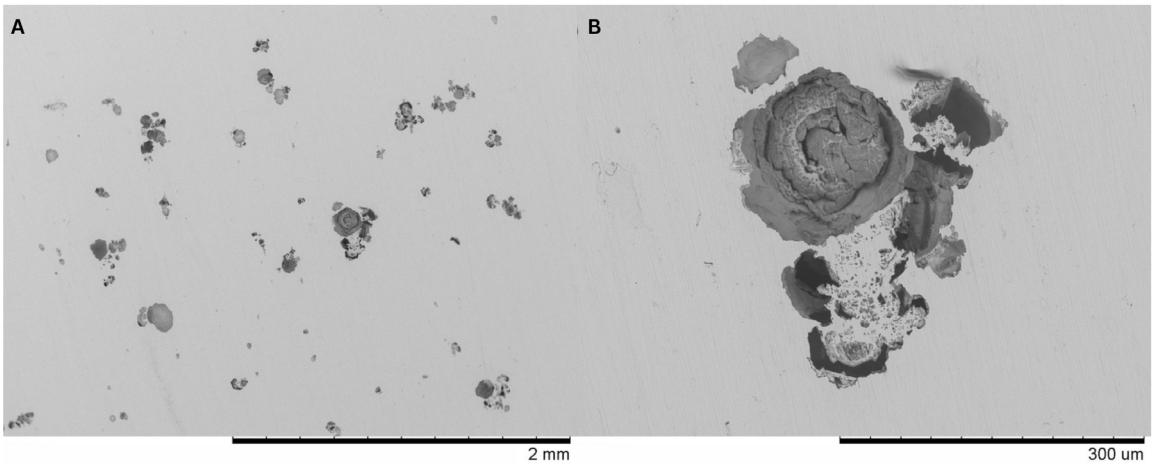

Figure 16. Characterization (SEM) of a sample of AISI 316 Steel after immersion for 30 days at 40 ºC. (a) 50x (b) 500x.

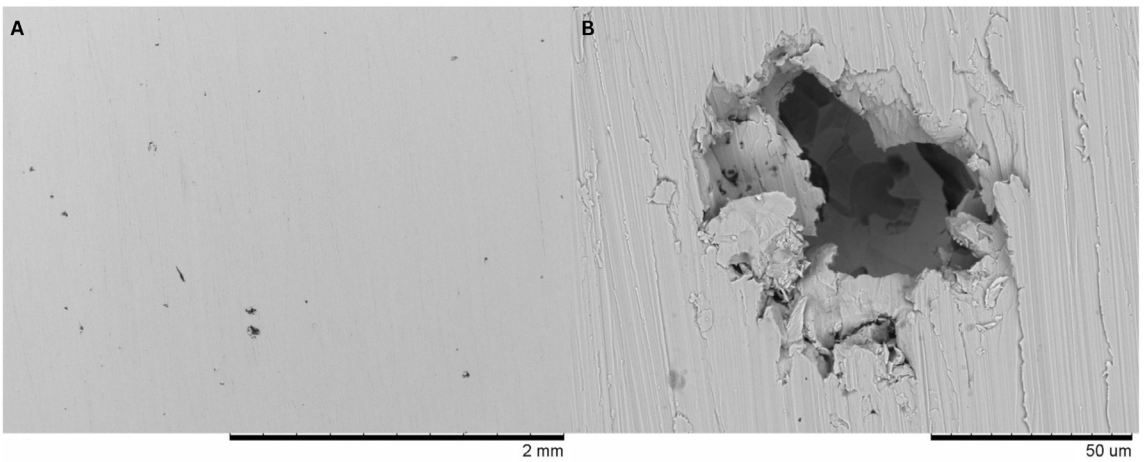

Figure 17. Characterization (SEM) of a sample of AISI 316 Steel after immersion for 30 days at 25 ºC. (a) 50x (b) 500x.

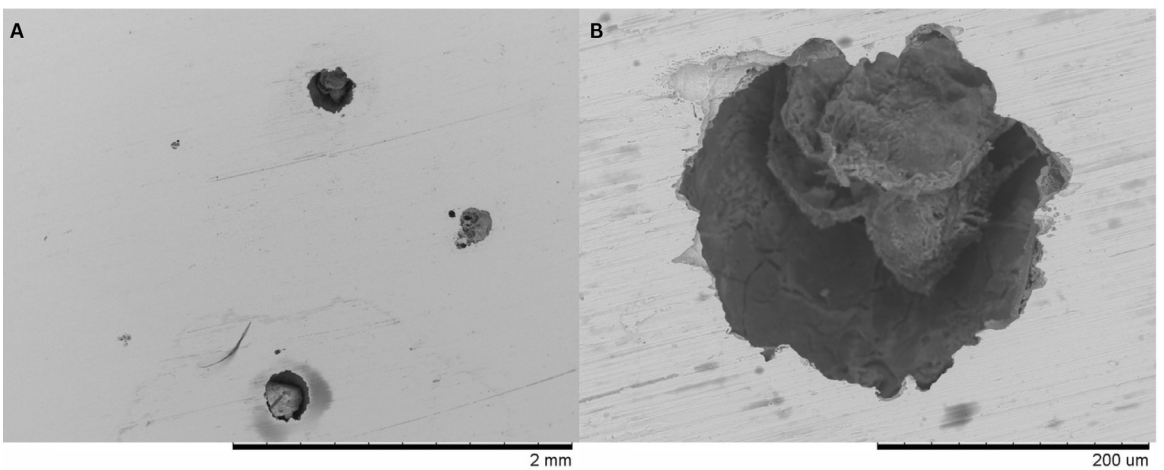

Figure 18. Characterization (SEM) of a sample of AISI 304 Steel after immersion for 30 days at 40 ºC. (a) 50x (b) 500x.

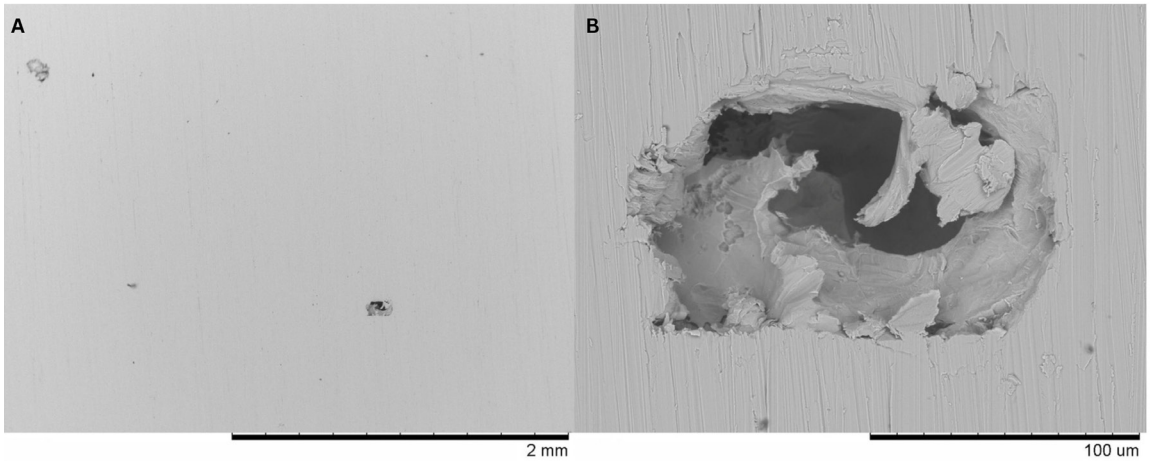

Figure 19. Characterization (SEM) of a sample of AISI 304 Steel after immersion for 30 days at 25 ºC. (a) 50x (b) 500x.

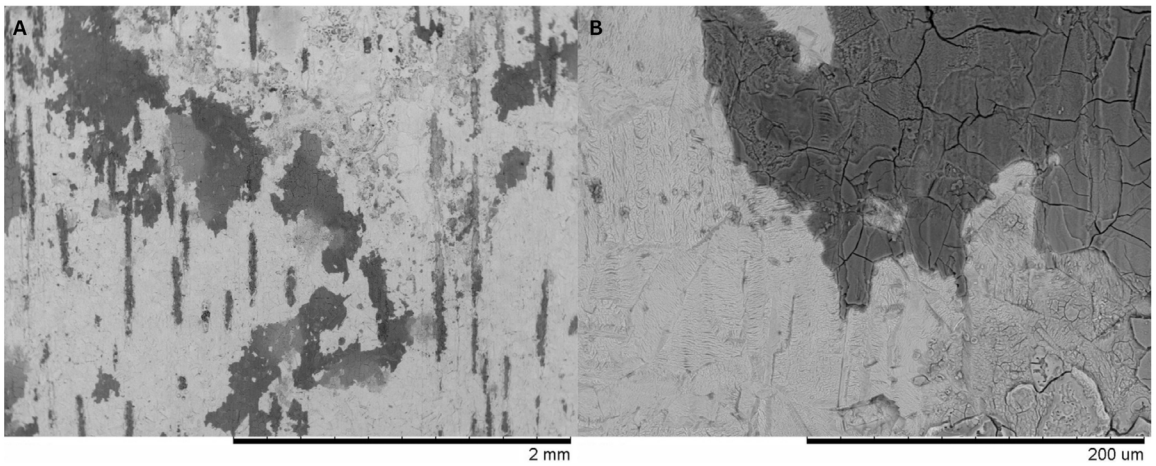

Figure 20. Characterization (SEM) of a sample of Monel 400 after immersion for 30 days at 40 ºC. (a) 50x (b) 500x.

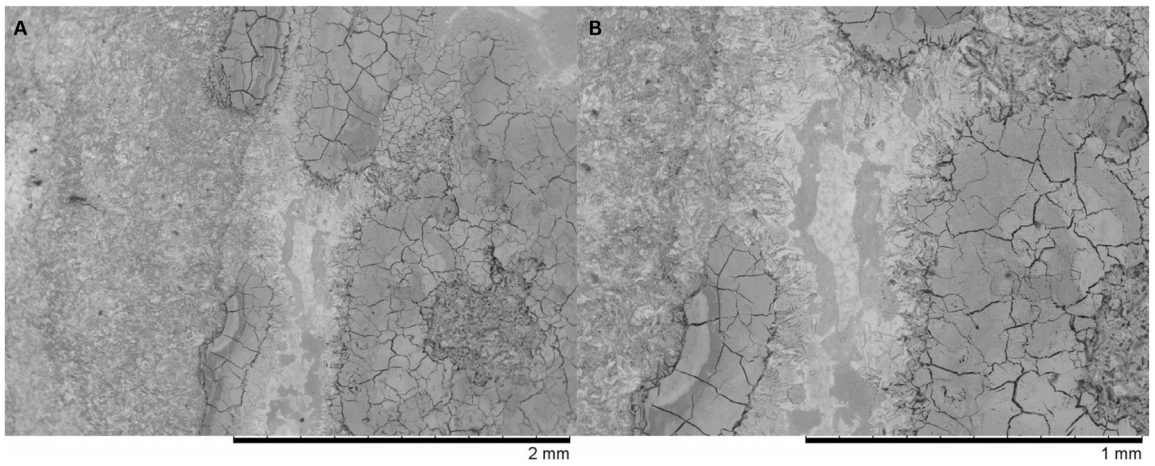

Figure 21. Characterization (SEM) of a sample of Monel 400 after immersion for 30 days at 25 ºC. (a) 50x (b) 500x.

according to Table 15, Titanium did not show signs of localized corrosion after 30 days in immersion.

Studies show that the excellent corrosion resistance of titanium is mainly due to the presence of a very stable oxide film (TiO_2) on its surface[14,15]. This oxide layer is extremely thin, only a few nanometres thick, but it is highly resistant to corrosion. The oxide layer forms spontaneously in the presence of oxygen.

According to Lei[16] the International Industrial Chimney Committee (ICIC), recommends the use of pure titanium as an insert material in the chimney design of coal-fired power plants, since pure titanium can resist in a strongly acid medium (mixture of sulfuric acid, nitric acid and hydrochloric acid).

Hastelloy C276 and Inconel 625 showed very similar behaviour at 40 ºC both in the anodic polarization (Figure 22) and in the immersion tests in which they did not show signs of localized corrosion after 30 days (Table 15).

Both alloys have high concentrations of chromium (14.5% to 16.5% and 21% respectively) and molybdenum (15% to 17% and 9% respectively). When exposed to air or water, chromium reacts with oxygen to form a thin, invisible layer of chromium oxide. This oxide layer is highly adherent, meaning that it adheres tightly to the metal surface and provides an additional corrosion barrier. The oxide layer that forms on chromium is self-repairing. If the oxide layer is damaged, for example by scratching or scraping, the chromium in the metal reacts with oxygen to form a new oxide layer.

Molybdenum is one of the main alloying elements that are related to the pitting corrosion resistance of stainless steels[17]. Some researchers[17,18] have discussed that the formation of Molybdenum oxides in films or inside pit walls can effectively increase corrosion resistance. The beneficial effects of molybdenum can be interpreted in terms of the decrease in active surface sites by the formation of molybdenum oxide at these sites.

The variations in molybdenum concentrations between Hastelloy C276 and Inconel 625 are more pronounced than those in chromium concentrations, reaching 8% and 6.5% respectively. Several factors could account for the equivalent performance of these materials despite these discrepancies.

As per Lei et al.[16], multiple metallic alloys demonstrated superior resistance to pitting corrosion in solutions containing bromide, such as DBNPA, compared to those containing chlorides when the molybdenum content was lower (2%). This trend reversed when the molybdenum content increased (5% and 10%), potentially mitigating the impact generated by the difference in molybdenum concentration.

Inconel 625 has 0.27% by weight of titanium and 0.06% of carbon, which enables the formation of TiC[19]. Rodrigues et al.[20]demonstrates that Ti used as a stabilizer and refiner element positively affects the mechanical properties and corrosion resistance by forming very stable particles such as TiC, considered one of the most suitable reinforcement materials for improving properties mechanical and corrosion resistance.

Under the condition of 40 ºC, Superduplex steel SAF 2507 exhibited the smallest passive domain, which was approximately 50% less than that of Inconel 625 and Hastelloy C276. Despite its high chromium concentration (25%), SAF 2507 has a lower molybdenum content (4%). Moreover, it is characterized by a ferritic matrix, in contrast to the nickel matrix found in Inconel 625 and Hastelloy C276. In the galvanic series, ferrite is less noble than nickel, implying that ferrite is more susceptible to electron loss and subsequent corrosion when exposed to corrosive environments[17].

According to Figure 23, among the metals that exhibited active dissolution, Duplex steels SAF 2205, AISI 317, and AISI 347 were the ones that achieved the lowest current densities at 100 mV above the corrosion potential. In contrast, other steels displayed higher densities, around 10^{-04}, suggesting a more rapid corrosion process. The observed difference between Duplex SAF 2205 steel and AISI 321 steel, for instance, can be attributed to the substantial presence of Molybdenum and a higher concentration of Chromium in Duplex SAF 2205 steel, which are known to enhance corrosion resistance.

Duplex 2205, is noteworthy for its performance in the 30-day immersion tests. Despite not demonstrating a passivation domain at a temperature of 40 ºC, Duplex 2205 did not exhibit any signs of localized corrosion. This behaviour could be indicative of a couple of scenarios. One possibility is that the material's Open Circuit Potential (OCP), a measure of the potential difference between a metal electrode and its

Table 15. Incidence and density of pits (immersion test).

Alloy	Pit Density	
	25 ºC	40 ºC
Titanium Grade 2	Passivation	Passivation
Inconel 625	Passivation	Passivation
Hastelloy c276	Passivation	Passivation
Superduplex 2507	Passivation	Passivation
Duplex 2205	Passivation	Passivation
ASIS 347	1.7 x 106 pit/m^2	6.25 x 105 pit/m^2
AISI 321	2.84 x106 pit/m^2	1.25 x 105 pit/m^2
AISI 317	Passivation	1.0 x 105 pit/m^2
AISI 316	6.1 x 106 pit/m^2.	3.1 x 105 pit/m^2
AISI 304	1.25 x 105 pit/m^2	3.7 x 105 pit/m^2
Monel 400	Generalized corrosion	Generalized corrosion

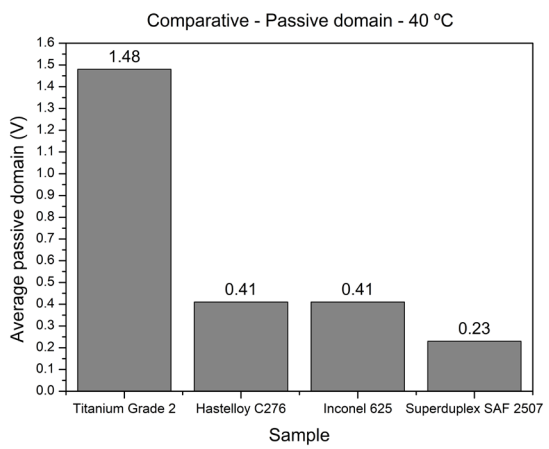

Figure 22. Passive domain at 40 ºC.

solution when no current flows to or from it, is close to its corrosion potential. In other words, the material might be in a state of equilibrium with its environment, which could prevent the onset of corrosion.

Another explanation could be related to the duration of the test. The 30-day period may not have been sufficient for the emergence of localized corrosion points. Corrosion is a time-dependent phenomenon, and the initiation and propagation of corrosion sites can sometimes take longer periods, depending on the material and the environmental conditions[21].

When comparing the chemical compositions of Superduplex SAF 2507, which achieved a passive domain, and Duplex SAF 2205, which underwent dissolution, it is evident that Superduplex SAF 2507 contains 3% more Chromium and 1% more Molybdenum. This suggests a superior resistance to corrosion in comparison to Duplex SAF 2205 steel.

Analysing the density of pits at 40 ºC, the lowest densities, around 10^5 pits per square meter, belong to the steels that have more chromium in their composition, AISI 317 and AISI 304, which have around 1% of chromium more than the others. Sabará[1] studying differences in the corrosion resistance of stainless steels, reached results that demonstrate that differences of 1% in the concentration of chromium in these steels can produce significant effects on their resistance to corrosion.

According to Figure 24, it is possible to observe that the alloys Hastelloy C276, Superduplex SAF 2507 and Inconel 625 obtained the largest passive domains for the 25 ºC condition. AISI class stainless steels (317, 304 and 316) and Duplex SAF 2205 have similar passive domains at room temperature. Figure 25 shows the 3 alloys that showed active dissolution at 25 ºC, these being AISI 347, AISI 321 and Monel 400.

Among the nickel alloys, there is a great discrepancy in the corrosion resistance of Hastelloy C276 and Inconel 625 alloys when compared to Monel 400. Checking Table 1, it is observed the significant presence of chromium and molybdenum in Hastelloy C276 and Inconel 625 alloys, which does not occur for Monel 400, which has a high concentration of copper, thus explaining the observed difference. Copper additions improve the mechanical properties of steels and can improve corrosion resistance and weldability properties, however the absence of chromium and molybdenum in the composition of Monel 400 was a detrimental factor.

Despite different chemical compositions Hastelloy C276 and Inconel 625 obtained similar results. According to Table 1, Hastelloy C276 has 14.5 to 16.5% of Chromium and 15 to 17% of Molybdenum, while Inconel 625 has 21% of Chromium, 9% of Molybdenum and 3.5% of Niobium. The addition of Niobium may be the reason why even with lower Molybdenum concentration Inconel 625 almost matched Hastelloy C276 in the tested condition.

Among the stainless steels, the Superduplex SAF2507 stands out due to its corrosion resistance, which has the highest passivation domain of stainless steels. The Duplex SAF 2205 obtained a result like the AISI class. Analysing Table 2, it is possible to observe that Superduplex SAF 2507 has the highest concentration of Chromium and Molybdenum among the other steels, which explains its greater field of passivation.

The only AISI grade steels that did not passivate in this condition were the AISI 321 and AISI 347 alloys, which can be attributed to the fact that they do not contain Molybdenum and have the lowest concentrations of Chromium in their compositions.

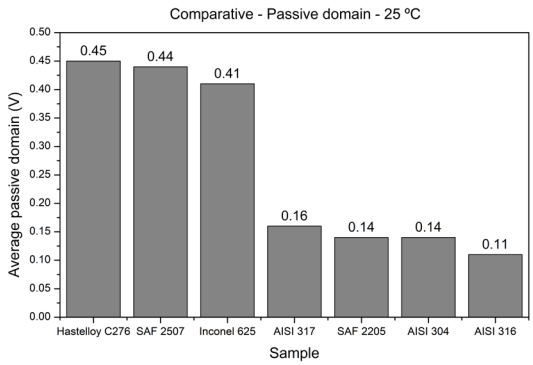

Figure 24. Passive domain at 25 ºC.

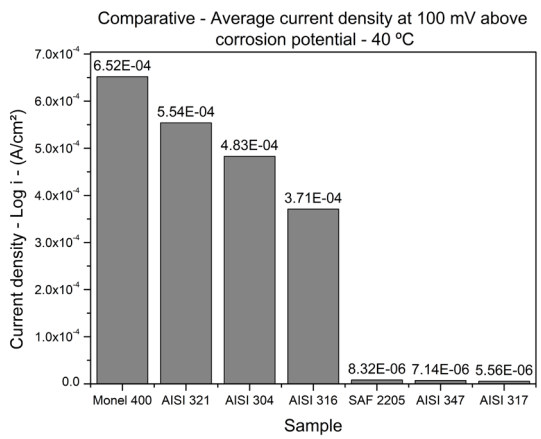

Figure 23. Average current density at 100 mV above corrosion potential at 40 ºC.

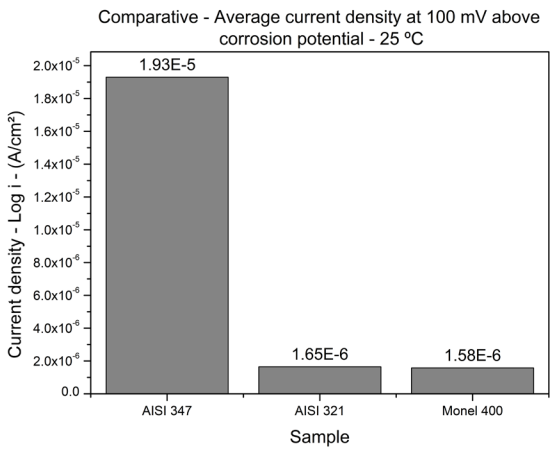

Figure 25. Average current density at 100 mV above corrosion potential at 25 ºC.

Table 16. PREN values of the analysed alloys.

Titanium Grade 2	--
Hastelloy C276	74.5
Inconel 625	50.7
Superduplex SAF 2507	43.0
Duplex SAF 2205	35.9
AISI 347	18.3
AISI 321	18.0
AISI 317	30.6
AISI 316	25.3
AISI 304	19.0
Monel 400	--

Table 17. Average passivation domain obtained from anodic polarization curves at 40 ºC in 100% BDNPA biocide solution.

Average passivation domain obtained from anodic polarization curves at 40 ºC in 100% BDNPA biocide solution. (V) |Pitting potential| – |Corrosion Potential|	
Titanium Grade 2	1.48
Hastelloy C276	0.41
Inconel 625	0.41
Stainless Steel Superduplex SAF 2507	0.23

6. Pren Comparison Proposal

The Pitting Resistance Equivalent Number (PREN) is a theoretical predictive measurement that provides an estimation of the resistance of an alloy to pitting corrosion. It was proposed as an index to classify the pitting corrosion resistance of corrosion-resistant alloys[1]. The PREN is calculated using a mathematical formula specified by the ISO 15156–3 standard. This formula considers the percentages of key alloying elements such as Chromium, Molybdenum, and Nitrogen, which are known to enhance the corrosion resistance of the alloy.

The PREN serves as a useful tool in material selection, particularly in applications where pitting corrosion is a concern. A higher PREN-value indicates a higher resistance to localized pitting of the stainless steel[22]. A common PREN formulation is expressed as following:

$$PREN = \%Cr + 3,3x\left(\%Mo + 0,5x\%W\right) + 16x\%N$$

The coefficients associated with different alloying elements provide a measure of the relative significance of these elements in augmenting the resistance to pitting. The environment considered by the standard is in the presence of dissolved chlorides and oxygen, such as sea water. In this context, an evaluation of the investigated alloys is presented. This evaluation is intended solely for comparison purposes, providing a basis for understanding the relative performance of different alloys in a standardized environment.

It is observed that Titanium Grade 2 and Monel 400 yielded zero values. These alloys do not exhibit substantial values of the alloying elements Tungsten (W), Nitrogen (N), Chromium (Cr), and Molybdenum (Mo) in their chemical compositions, rendering them non-comparable using the Pitting Resistance Equivalent Number (PREN).

As per the data presented in Table 16 and Figures 22 and 23, a correlation was identified between PREN and the analysed alloys. The ranking mirrored the results obtained from the immersion and anodic polarization tests. Future research could potentially focus on this correlation with the objective of utilizing PREN as a benchmark for the selection of materials suitable for the transportation and storage of 100% BDNPA biocide solution.

7. Conclusion

During the development of this work, it became clear that the analysis of the corrosivity of biocides is a major gap in the literature. There are few studies investigating the interaction between biocides and metals that are commonly used in industry. The focus of study has been the degradation of biocides in the environment and their effectiveness against microbiologically induced corrosion.

Among the analysed alloys, only 4 were approved by the tests in all tested temperature ranges (Titanium Grade 2, Hastelloy C276, Inconel 625 and Superduplex Steel SAF 2507). These alloys did not present a localized corrosion process in any of the 30-day immersion tests, in addition, they obtained a significant passivation domain in the anodic polarization test at 40 ºC. Thus, Table 17 brings the ranking of materials according to the passive domain presented at a temperature of 40 °C.

8. Acknowledgments

This work was funded by the following projects CNPq (405505/2021-3), FAPEMIG (APQ-02540-21).

9. References

1. Sabará CVL, Prachedes LNS, Santos LC, Sabará MA, Souza RC, Sene AF, et al. Influence of parameters related to microstructure, chemical composition and environment characteristics on localized corrosion failure susceptibility of supermartensitic stainless steels. Eng Fail Anal. 2021;127:24.
2. Bowman E, Thompson N, Gl D, Moghissi O, Gould M, Payer J. Assessment of the global cost of corrosion. Houston: NACE International; 2016.
3. Wasim M, Djukic MB. External corrosion of oil and gas pipelines: a review of failure mechanisms and predictive preventions. J Nat Gas Sci Eng. 2022;100:104467.
4. Liu H, Cheng YF. Corrosion of initial pits on abandoned X52 pipeline steel in a simulated soil solution containing sulfate-reducing bacteria. J Mater Res Technol. 2020;9(4):7180.
5. Wang D, Ramadan M, Kumseranee S, Punpruk S, Gu T. Mitigating microbiologically influenced corrosion of an oilfield biofilm consortium on carbon steel in enriched hydrotest fluid using 2,2-dibromo-3-nitrilopropionamide (DBNPA) enhanced by a 14-mer peptide. J Mater Sci Technol. 2020;57:146.
6. Kahrilas GA, Blotevogel J, Stewart PS, Borch T. Biocides in hydraulic fracturing fluids: A critical review of their usage, mobility, degradation, and toxicity. Environ Sci Technol. 2015;49:16.
7. Blanchard FA, Gonsior SJ, Hopkins DL. 2,2-Dibromo-3-nitrilopropionamide (DBNPA) chemical degradation in natural waters: experimental evaluation and modeling of competitive pathways. Water Res. 1987;21(7):7

8. Shi X, Zhang R, Sand W, Mathivanan K, Zhang Y, Wang N, et al. Comprehensive Review on the Use of Biocides in Microbiologically Influenced Corrosion. Microorganisms. 2023;11:24.
9. Prachedes LNS, Sabará CVL, Santos LC, Souza RC, Caldeira L, Vaz GL, et al. Evaluation of Cr, Mo, Ti and Cu on the pitting corrosion resistance of supermartensitic stainless steels at different temperatures - 2021. In: *21st International Corrosion Congress, ICC INTERCORR WCO 2021*. Proceedings. Rio de Janeiro: ABRACO; 2021. p. 15.
10. Santos BAF, Serenario MED, Souza RC, Santos LC, Oliveira JR, Vaz GL, et al. The electrolyte renewal effect on corrosion and scales formation of API X65 carbon steel immersed in condensed water environments. In: *21st International Corrosion Congress, ICC INTERCORR WCO 2021*. Proceedings. Rio de Janeiro: ABRACO; 2021. p. 15.
11. Eriksson J-E, Lehmusto J, Dirbeba M, Silvander L, Lindberg D, Hupa L. The effect of Cl, Br, and F on high-temperature corrosion of heat-transfer alloys. Fuel. 2023;348:128516.
12. Campa MF, Techtmann SM, Ladd MP, Yan J, Patterson M, Amaral AGM, Carter KE, et al. Surface water microbial community response to the biocide 2,2-dibromo-3-nitrilopropionamide, used in unconventional oil and gas extraction. Appl Environ Microbiol. 2019;85(21):e01336-19.
13. Wu B, Xiu J, Yu L, Huang L, Yi L, Ma Y. Research advances of microbial enhanced oil recovery. Heliyon. 2022;8(11):e11424.
14. Dubent S, Mazard A. Characterization and corrosion behaviour of grade 2 titanium used in electrolyzers for hydrogen production. Int J Hydrogen Energy. 2019;44:15622.
15. Harada R, Takemoto S, Kinoshita H, Yoshinari M, Kawada E. Influence of sulfide concentration on the corrosion behavior of titanium in a simulated oral environment. Mater Sci Eng C. 2016;62:268.
16. Lei L, Sun Y, Zheng K, Wang X, He P, Liu Y, et al. A comparative study on the critical pitting criteria of a super ferritic stainless steel at different temperatures in chloride or bromide solution. Corros Sci. 2021;183:14.
17. Jung K, Ahn S, Kim Y, Oh S, Ryu W-H, Kwon H. Alloy design employing high Cr concentrations for Mo-free stainless steels with enhanced corrosion resistance. Corros Sci. 2018;140:61.
18. Habazaki H, Kawashima A, Asami K, Hashimoto K. The corrosion behavior of amorphous Fe-Cr-Mo-P-C and Fe-Cr-W-P-C alloys in 6 M HCl solution. Corros Sci. 1992;33(2):225.
19. Bakkar A, Ahmed MMZ, Alsaleh NA, Seleman MMES, Ataya S. Microstructure, wear, and corrosion characterization of high TiC content Inconel 625 matrix composites. J Mater Res Technol. 2019;8(1):1102.
20. Rodrigues CAD, Pagotto JF, Motheo AJ, Tremiliosi-Filho G. The effect of titanium on pitting corrosion resistance of welded supermartensitic stainless steel. Corros Eng Sci Technol. 2017;52(2):141.
21. Lazareva A, Owen J, Vargas S, Barker R, Neville A. Investigation of the evolution of an iron carbonate layer and its effect on localized corrosion of X65 carbon steel in CO2 corrosion environments. Corros Sci. 2021;192:10.
22. Chen D, Dong C, Ma Y, Ji Y, Gao L, Li X. Revealing the inner rules of PREN from electronic aspect by first-principles calculations. Corros Sci. 2021;189:13.